Solvent and Spectral Effects in the Ultrafast Charge Recombination Dynamics of Excited Donor−Acceptor Complexes

Serguei V. Feskov, Vladimir N. Ionkin, and Anatoly I. Ivanov*

Department of Physics, Volgograd State University, University Avenue 100, Volgograd 400062, Russia

Hans Hagemann and Eric Vauthey*

Department of Physical Chemistry, University of Geneva, 30 Quai Ernest Ansermet, CH-1211 Geneva 4, Switzerland

Received: October 1, 2007; In Final Form: October 28, 2007

The charge recombination dynamics of excited donor−acceptor complexes consisting of hexamethylbenzene (HMB), pentamethylbenzene (PMB), and isodurene (IDU) as electron donors and tetracyanoethylene (TCNE) as electron acceptor in various polar solvents has been investigated within the framework of the stochastic approach. The model accounts for the reorganization of intramolecular high-frequency vibrational modes as well as for the solvent reorganization. All electron-transfer energetic parameters have been determined from the resonance Raman data and from the analysis of the stationary charge transfer absorption band, while the electronic coupling has been obtained from the fit to the charge recombination dynamics in one solvent. It appears that nearly 100% of the initially excited donor−acceptor complexes recombine in a nonthermal (hot) stage when the nonequilibrium wave packet passes through a number of term crossings corresponding to transitions toward vibrational excited states of the electronic ground state. Once all parameters of the model have been obtained, the influence of the dynamic solvent properties (solvent effect) and of the carrier frequency of the excitation pulse (spectral effect) on the charge recombination dynamics have been explored. The main conclusions are (i) the model provides a globally satisfactory description for the IDU/TCNE complex although it noticeably overestimates the spectral effect, (ii) the solvent effect is quantitatively well described for the PMB/TCNE and HMB/TCNE complexes but the model fails to reproduce their spectral effects, and (iii) the positive spectral effect observed with the HMB/TCNE complex cannot be described within the framework of two-level models and the charge redistribution in the excited complexes should most probably be taken into account.

I. Introduction

Photoexcitation in the charge-transfer band of donor−acceptor complexes (DACs) triggers a series of processes shown in the following scheme:

$$\begin{array}{ccc} D^+A^- & \xrightarrow{\varphi} & D^+ + A^- \\ h\nu \uparrow\downarrow k_{CR} & & \\ DA & & \end{array} \qquad (1.1)$$

where $h\nu$ indicates the photoexcitation of the ground-state complex (DA) leading to the population of the excited (charge separated) state (D^+A^-), k_{CR} is the charge recombination (CR) rate constant, and φ is the free ion quantum yield. Since charge recombination of excited DACs in polar solvents is in most cases ultrafast,[1−9] the free ion quantum yield is negligibly small.

Investigations of ultrafast CR have uncovered the substantial role of nuclear nonequilibrium in such processes.[9−13] Indeed, in ultrafast CR the nonequilibrium initial nuclear state produced by the pump pulse relaxes in parallel with its chemical transformation, so that the reaction proceeds in a nonequilibrium regime. In this case, a dependence of the effective CR rate constant on the excitation pulse carrier frequency (the spectral effect) may be expected. Both experimental and theoretical investigations have shown the spectral effect to be relatively small but still reliably observable.[14−17]

The second important peculiarity of ultrafast CR in excited DACs is the absence of the normal Marcus regime, that is, the regime where the rate constant increases with increasing the reaction driving force provided the latter is smaller than reorganization energy. Indeed, a monotonous decrease of the CR rate with driving force has experimentally been observed and reported in a series of papers by Mataga and cowokers.[1−3] This measured dependence can however not be explained within the standard equilibrium nonadiabatic Marcus theory that predicts a bell-shaped dependence of the rate on the CR driving force. Nevertheless, such a non-Marcus behavior was explained later within the framework of both equilibrium Frantsuzov−Tachiya theory,[18] where CR is assumed to be a transition between the excited and ground adiabatic electronic states of the DAC induced by the nonadiabaticity operator and the nonequilibrium nonadiabatic theories accounting for transitions to a number of vibrational sublevels of the ground electronic state involving high-frequency modes.[9,19]

The third feature of ultrafast CR is the important role of intramolecular modes.[11,12,20−22] It has been known for a long time that these modes can increase the rate constant of highly exergonic electron-transfer reactions by several orders, but on

* Corresponding authors. E-mail: physic@vlink.ru (A.I.I.) and Eric.Vauthey@chiphy.unige.ch (E.V.).

10.1021/jp709587x CCC: $40.75 © 2008 American Chemical Society
Published on Web 01/09/2008

the other hand, they can even suppress the rate of weakly exergonic reactions. This however is only true for thermal reactions. It was recently shown that high-frequency vibrational modes can also profoundly accelerate weakly exergonic nonequilibrium CR.[12,19,23] In these reactions, the initial excited-state wave packet passes during its relaxation through the multiple term crossings undergoing hot transitions at each of them, so the wave packet may disappear before its equilibration. This leads to a great reduction of the CR time constant. An important feature of this model is that the CR dynamics are predicted to be nearly exponential in accordance with the majority of experimental data and in contrast to most nonequilibrium theories.

It should also be noted that there is a pronounced dependence of the effective CR rate constant on the dynamic characteristics of the solvent even in cases when the shape and maximum of the charge transfer absorption band varies very weakly with the solvent.[17] The last experimental fact is an indication that the medium reorganization energy is practically independent of the solvent and, hence, the solvent effect is mainly due to dynamic solvent properties. In spite of the fact that very detailed experimental and theoretical explorations of the CR kinetics have been performed with a large number of DACs, there are still several unresolved issues regarding the mechanism of ultrafast CR of excited DACs. One of the most important questions is the reaction regime that is realized in a specific DAC. Indeed, a successful quantitative description of the CR rate constants can be obtained both in the weak[9,11,12,2] and the strong electronic coupling limits.[6,18] This fact clearly indicates that a good fit to the experimental rate constants within the framework of a specific theory is not a reliable evidence of its validity. A more rigorous test of the model should include the reproduction of at least a few dependencies of the rate constants on parameters that can be varied over a sufficiently large range.

Recently, the ultrafast CR dynamics of a series of the DACs consisting of hexamethylbenzene (HMB), pentamethylbenzene (PMB), and isodurene (IDU) as electron donors and tetracyanoethylene (TCNE) as electron acceptor in the series of polar solvents acetonitrile (ACN), valeronitrile (VaCN), and octanenitrile (OcCN) characterized by a more than tenfold increase of the diffusional relaxation time have been experimentally investigated.[17] The effective CR time constants of all DACs have been shown to decrease markedly with the diffusive relaxation time of the solvent. For the sake of brevity, this dependence will be called hereafter the solvent effect. In slowly relaxing solvents, the effective CR rate constant in some DACs was also found to depend on the excitation wavelength, that is, to exhibit a spectral effect. It has been found that the solvent effect was very similar for all three DACs investigated, while the spectral effect was DAC dependent. In VaCN, the spectral effect, measured between 480 and 620 nm, was negative (decrease of the CR rate with increasing excitation pulse frequency) with IDU/TCNE, positive with HMB/TCNE, and vanishingly small with PMB/TCNE.[17]

The main aim of this paper is to reproduce within the framework of a single model (i) the charge transfer absorption band, (ii) the CR dynamics for a single excitation pulse carrier frequency in a single solvent, (iii) the spectral effect, and (iv) the solvent effect. All free parameters of the model will be fixed during the two initial steps i and ii. As a consequence, steps iii and iv will be serious tests of the model.

II. The Model

The description of ultrafast charge recombination of DACs in a polar solvent is commonly based on the assumption that only two electronic states of the complex participate in the charge separation and recombination processes: the neutral ground state $|g\rangle$ and the excited ionic state $|e\rangle$. The system, initially in the ground state with a thermal distribution of nuclear coordinates, is transferred to the excited state $|g\rangle \rightarrow |e\rangle$ by a short pump pulse (see Figure 1.)

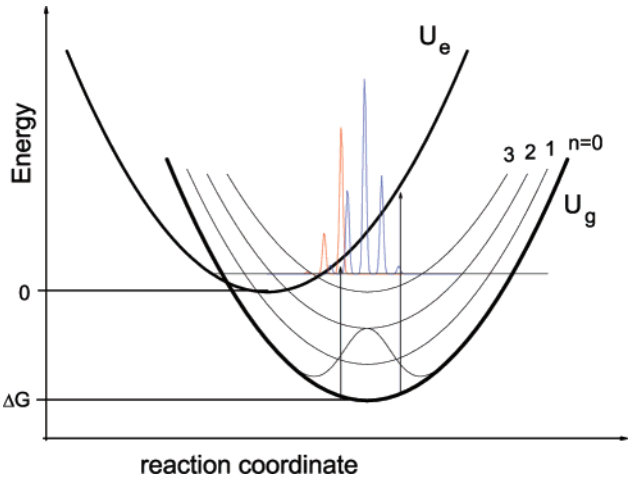

Figure 1. Cuts in the free energy surface of the ground and the excited states of a DAC. The thin curves represent vibrational excited states of the ground electronic state. The initial distributions along the reaction coordinate correspond to lower frequency (red) and higher frequency (blue) excitation pulses of 100 fs duration.

The distribution of the population transferred on the excited-state surface depends on the spectral characteristics of the pump pulse, an example being illustrated in Figure 1. The population of this state, being in nonequilibrium, is subjected to a series of relaxation processes: the reorganization of solvent and intramolecular vibrational degrees of freedom are of primary importance among them.[24] Defining the reaction coordinate of CR as a difference between the corresponding energy levels $\Delta E(t) = E_g - E_e$, one can describe the solvent relaxation through the autocorrelation function $K(t) = \langle \Delta E(t) \Delta E(0) \rangle$.[25,26] For the Debye model of solvent relaxation, this function is written in the form[25]

$$K(t) = 2E_{rm} k_B T X(t) \tag{2.1}$$

where E_{rm} is the solvent reorganization energy, k_B is the Boltzmann constant, T is the temperature, $X(t) = e^{-t/\tau_L}$, and τ_L is the longitudinal dielectric relaxation time. The exponential form of $K(t)$ implies that the relaxation process is Markovian. In this case, the motion along the reaction coordinate is diffusive and can be described by the Smoluchowski operator.

The real solvents are characterized by several relaxation time scales. These time scales are attributed to different relaxation modes corresponding to distinct types of motions of the solvent molecules. If the relaxation modes are independent as usually assumed, then the autocorrelation function $K(t)$ is a sum of contributions from each mode.

Using the Markovian approximation for all solvent modes, one can write $K(t)$ in the same form as in eq 2.1 but with the solvent relaxation function, $X(t)$, as a sum of exponentials[27,25]

$$X(t) = \sum_1^N x_i \, e^{-t/\tau_i} \tag{2.2}$$

Here, $x_i = E_{ri}/E_{rm}$, τ_i, and E_{ri} are the weight, the relaxation time constant, and the reorganization energy of the ith medium mode, respectively; $E_{rm} = \sum E_{ri}$, and N is the number of solvent modes.

However, in real polar solvents, the exponential stage of the autocorrelation function decay is only achieved at long times. A considerable part of decay is not diffusive but rather inertial.[28−31] The initial relaxation, being inertial in nature, is described with a Gaussian autocorrelation function $x_1\ e^{-(t/\tau_1)^2}$. In this case, the solvent relaxation function becomes $X(t) = x_1\ e^{-(t/\tau_1)^2} + \sum_2^N x_i\ e^{-t/\tau_i}$. The exponential and Gaussian correlations reflect essentially different types of motion along the reaction coordinate that can lead to a difference in the reaction dynamics. In the case of strong electron transfer, this difference can be substantial. However, in the case of weak electron transfer when the Golden rule is applicable, the reaction rate constant does not depend at all on the dynamic properties of the solvent. For the systems considered here, the excitation pulse produces a wave packet in the region of extremely weak sinks. In this case, one might expect the CR dynamics at the initial relaxation stage to depend on the inertial mode time scale but not on the particular type of the motion along the reaction coordinate. This allows the whole relaxation process to be described in terms of several diffusive modes. Henceforward, we shall approximate the solvent relaxation function with eq 2.2.

The diabatic free energy surfaces for the electronic states along the coordinates Q_i are

$$U_g^{(n)} = \sum \frac{Q_i^2}{4E_{ri}} + \sum_\alpha n_\alpha \hbar\Omega_\alpha + \Delta G_{CR}$$

$$U_e = \sum \frac{(Q_i - 2E_{ri})^2}{4E_{ri}} \quad (2.3)$$

where Ω_α is the frequency of the αth intramolecular quantum mode, n_α ($n_\alpha = 0, 1, 2, ...$) is the quantum number of αth mode (the number of vibrational sublevels), and ΔG_{CR} is the CR free energy. The terms intersect along the lines $\sum Q_i = z = z_n^\dagger$, where $z_n^\dagger = E_{rm} - \Delta G_{CR} - \sum_\alpha n_\alpha \hbar\Omega_\alpha$. Obviously, the quantity $z_n^\dagger$ may be considered as a position of a sink along the reaction coordinate $Q = \sum Q_i$. Although this position is determined by the set of quantum numbers $\{n_\alpha\}$, the sinks can be numbered. It implies that the set $\{n_\alpha\}$ is mapped in a one-to-one way onto the set of whole numbers n. The correspondence is fixed by the inequality $z_n^\dagger < z_{n+1}^\dagger$.

Thus, we are led to the problem of nonequilibrium electronic transitions. This is a long-standing problem which has been already addressed from different points of view.[10,14,32,44] Here, we need an approach which could allow the CR dynamics to be simulated in the case of strong electron transfer when the nonthermal electron-transfer probability is significant. The stochastic point-transition approach[25] generalized to a multilevel system is well-suited to this goal.

Within this approach, the temporal evolution of the system can be described by a set of differential equations for the probability distribution functions for the excited state $\rho_e(\mathbf{Q},t)$ and for the nth sublevel of the ground state $\rho_g^{(n)}(\mathbf{Q},t)$

$$\frac{\partial \rho_e}{\partial t} = \hat{L}_e \rho_e - \sum_n k_n(\mathbf{Q})\,(\rho_e - \rho_g^{(n)}) \quad (2.4)$$

$$\frac{\partial \rho_g^{(n)}}{\partial t} = \hat{L}_g \rho_g^{(n)} - k_n(\mathbf{Q})(\rho_g^{(n)} - \rho_e) + \sum_\alpha \frac{1}{\tau_v^{(n_\alpha+1)}} \rho_g^{(n'_\alpha)} - \frac{1}{\tau_v^{(n)}} \rho_g^{(n)} \quad (2.5)$$

where $\mathbf{Q}$ stands for the vector with components Q_1, Q_2, ..., Q_N, and $\hat{L}_g$ and $\hat{L}_e$ are the Smoluchowski operators describing diffusion on the U_g and U_e potentials

$$\hat{L}_g = \sum_{i=1}^N \frac{1}{\tau_i}\left[1 + Q_i \frac{\partial}{\partial Q_i} + \langle Q_i^2\rangle \frac{\partial^2}{\partial Q_i^2}\right] \quad (2.6)$$

$$\hat{L}_e = \sum_{i=1}^N \frac{1}{\tau_i}\left[1 + (Q_i - 2E_{ri}) \frac{\partial}{\partial Q_i} + \langle Q_i^2\rangle \frac{\partial^2}{\partial Q_i^2}\right] \quad (2.7)$$

with $\langle Q_i^2\rangle = 2E_{ri}k_BT$ being the dispersion of the equilibrium distribution along the ith coordinate. The coupling parameters $k_n(Q_1,Q_2,...,Q_N)$ are the Zusman rates of electron transfer between the excited state $|e\rangle$ and the nth vibrational sublevel of the ground state $|g\rangle$

$$k_n = \frac{2\pi V_n^2}{\hbar}\delta(U_e - U_g^{(n)}) = \frac{2\pi V_n^2}{\hbar}\delta(z - z_n^\dagger)$$

$$V_n^2 = V_{el}^2 F_n \qquad F_n = \prod_\alpha \frac{S_\alpha^{n_\alpha} e^{-S_\alpha}}{n_\alpha!} \quad (2.8)$$

where F_n is the Franck−Condon factor, $S_\alpha = E_{rv\alpha}/\hbar\Omega_\alpha$ and $E_{rv\alpha}$ are the Huang−Rhys factor and the reorganization energy of the αth high-frequency vibrational mode, respectively. The index n'_α stands for the set of quantum numbers $n'_\alpha = \{n_1,n_2,...n_\alpha + 1,...\}$. We adopt here a single-quantum mechanism of high-frequency mode relaxation and the transitions $n_\alpha \rightarrow n_\alpha - 1$ proceed with the rate constant $1/\tau_v^{(n_\alpha)}$. Naturally, the ground vibrational state is stable, and the equation $\tau_v^{(0)} = \infty$ must be fulfilled. In particular, this condition is met for the model $\tau_v^{(n_\alpha)} = \tau_v^{(1)}/n_\alpha$. The relaxation rate of the nth level is determined by the equation

$$\frac{1}{\tau_v^{(n)}} = \sum_\alpha \frac{1}{\tau_v^{(n_\alpha)}} \quad (2.9)$$

To specify the initial conditions, we assume that the pump pulse has a Gaussian form

$$E(t) = E_0 \exp\left\{i\omega_e t - \frac{t^2}{\tau_e^{\,2}}\right\} \quad (2.10)$$

and its duration τ_e is short enough to consider the medium frozen during excitation. This allows us to obtain the following general expression for the initial probability distribution function on the excited term[15]

$$\rho_e(\mathbf{Q}, t=0) = Z^{-1} \sum_{n_\alpha}\left[\prod_\alpha \frac{S_\alpha^{n_\alpha}\, e^{-S_\alpha}}{n_\alpha!}\right] \times \exp\left\{-\frac{(\hbar\delta\omega_e^{(n)} - \sum \tilde{Q}_i)^2 \tau_e^{\,2}}{2\hbar^2} - \sum \frac{\tilde{Q}_i^{\,2}}{4E_{ri}k_BT}\right\} \quad (2.11)$$

where $\tilde{Q}_i = Q_i - 2E_{ri}$, $\hbar\delta\omega_e^{(n)} = \hbar\omega_e + \Delta G_{CR} - E_{rm} - \sum_\alpha n_\alpha \hbar\Omega_\alpha$, and Z is a normalization factor.

Equation 2.11 shows the initial distribution, $\rho_e(\mathbf{Q}, t = 0)$, to be affected both by the excitation pulse carrier frequency, ω_e, and by the duration of the pumping pulse τ_e. This is clearly illustrated by Figure 1 where we display two initial distributions

calculated for the different excitation wavelengths 620 nm (red line) and 480 nm (blue line) used in the experiments.[17] We adopted here a model with a single high-frequency mode and the following set of parameters obtained from the fit to the charge transfer absorption band of the HMB/TCNE complex: $E_{rm} = 0.53$ eV, $\Delta G_{CR} = -1.74$ eV, $S = 2.72$, $\hbar\Omega = 0.17$ eV, and $\tau_e = 0.10$ ps. One can see a significant shift of the packets gravity centers along the reaction coordinate, as well as the internal pattern of the packets themselves. In fact, this pattern reflects the discreet energetic structure of the excited-state vibrational sublevels, and the peaks correspond to the excitation of a certain number of vibrational quanta. This structure is washed out both with increasing the number of active vibrational modes and with decreasing the pulse duration, τ_e, because of peaks overlapping. The shift of the wave packet centers has however a different physical origin and is almost independent of the number of vibrational modes.

The set of eqs 2.4 with the initial condition eq 2.11 was solved numerically using the Brownian simulation method.[15,45] We run 10^5 trajectories in order to obtain the necessary convergence of the results.

III. Simulation Results and Discussion

Fit to the Stationary Charge Transfer Absorption Band. In this section, the well-known fact that the CR of excited DAC is the reverse process to the charge-transfer excitation is used. This allows wealthy information on the CR parameters to be obtained from the charge-transfer absorption band spectrum.[6,7,11,46,47] The absorption spectrum was first analyzed with a model including a single accepting intramolecular mode of high frequency. The medium reorganization energy, the reaction free energy, the frequency, and the reorganization energy of the quantum mode were adjustable parameters. It appeared that different sets of parameters result in fits of the same quality. The only way to circumvent this difficulty was to reduce the number of free parameters. For example, the resonance Raman spectrum contains information on the intramolecular vibrational frequencies and their Franck−Condon factors. In ref 6, all parameters pertaining to the HMB/TCNE DAC were obtained from its resonance Raman spectrum and the fit to its stationary charge transfer absorption band. The same approach was applied here to the IDU/TCNE and PMB/TCNE DACs. Within the framework of the model used in this paper, the charge transfer absorption band is determined by the equation[5,11]

$$A = C\sum_{n_\alpha}\left[\prod_\alpha \frac{S_\alpha^{n_\alpha} e^{-S_\alpha}}{n_\alpha!}\right]\times \exp\left\{-\frac{[\Delta G_{CR} - E_r - \sum_\alpha n_\alpha\hbar\Omega_\alpha - \hbar\omega_e]^2}{4E_r k_B T}\right\} \quad (3.1)$$

where $E_r = E_{rm} + E_{cl}$ and E_{cl} is the reorganization energy of the intramolecular classical vibrational modes $\hbar\Omega_\alpha < k_B T$. The fit of eq 11 to the experimental charge transfer absorption bands with the resonance Raman data (intramolecular frequencies Ω_α and relative values of the Huang−Rhys factors S_α) allows E_r, ΔG_{CR}, and the absolute values of S_α to be determined.

The resonance Raman spectra of IDU/TCNE and PMB/TCNE have been measured in dichloromethane using two different experimental setups. In one case, the 568.2 nm line of a Ar/Kr laser was used; the sample solutions were located in a 1 cm quart cell, and the Raman signal was collected in backscattering geometry and dispersed with a Spex 1404 monochromator resulting in a 5 cm^{-1} spectral resolution. The second setup, using the 488 nm line of an Ar laser and with a 3 cm^{-1} spectral resolution, has been described in detail elsewhere.[48] The frequencies of the Raman lines were the same with both experimental setups, the only difference being that the DAC-to-solvent band intensities were substantially larger upon 568.2 nm irradiation, in agreement with the resonance effect. The resonance Raman spectrum of HMB/TCNE in carbon tetrachloride has been borrowed from refs 49 and 50. The resonance Raman intensities were supposed to be proportional to the Huang−Rhys parameters.

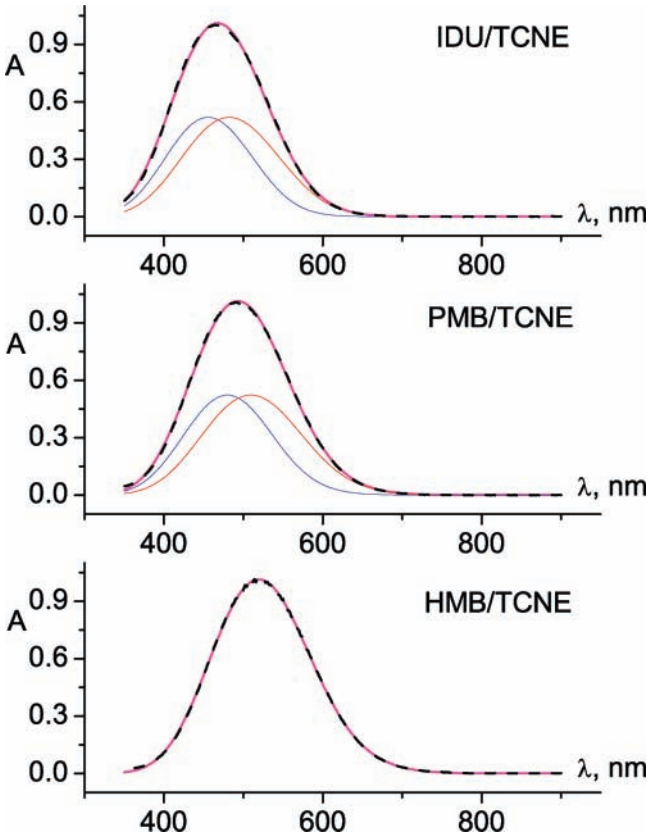

Figure 2. Stationary absorption spectra (black dashed lines) and best fit of the sum of two terms of the type of eq 3.1 (magenta solid lines). The two individual charge-transfer bands are plotted with red and blue thin lines.

It should be noted that all Raman active modes have to be divided into two groups: the classical modes $\hbar\Omega_\alpha < k_B T$ and the quantum modes $\hbar\Omega_\alpha > k_B T$. Only the total reorganization energy of all classical modes, namely, the sum of the intracomplex and the solvent reorganization energies, can be determined from the fit. Ten active quantum modes were found for each DAC. A single classical mode with frequency $\hbar\Omega_{11} = 0.021$ eV was extracted from the resonance Raman spectrum of HMB/TCNE and a total reorganization energy of 0.03 eV was obtained.[50] With both IDU/TCNE and PMB/TCNE, this mode was found at $\hbar\Omega_{11} = 0.020$ eV with a small reorganization energy of 0.020 eV.

The charge transfer absorption spectra of the IDU/TCNE and PMB/TCNE DACs are known to consist of two overlapping bands originating from the splitting of the two highest occupied molecular orbitals (HOMO) of the donors.[51,52] This splitting is very small and was set to 0.15 eV in the fit. The intensities of the two bands were supposed to be equal. In this case, the absorption band is approximated by the sum of two equations of the type of eq 11 differing only by the value of ΔG_{CR} (the

TABLE 1: Parameters Obtained from the Fit of the Sum of Two Terms of the Type of Eq 3.1 to the Stationary Absorption Spectra of the DACs in ACN[a]

	IDU/TCNE		PMB/TCNE		HMB/TCNE	
ΔG_{CR}	−1.749		−1.559		−1.521	
E_r	0.534		0.645		0.667	
	Ω_α	$E_{r\nu\alpha}$	Ω_α	$E_{r\nu\alpha}$	Ω_α	$E_{r\nu\alpha}$
1	0.0558	0.0017	0.0435	0.0007	0.0558	0.0060
2	0.0674	0.0031	0.0548	0.0013	0.0672	0.0008
3	0.0712	0.0033	0.0600	0.0016	0.0744	0.0016
4	0.0767	0.0012	0.0655	0.0014	0.1188	0.0077
5	0.1195	0.0028	0.0673	0.0014	0.1602	0.0321
6	0.1428	0.0044	0.0742	0.0012	0.1722	0.0136
7	0.1608	0.0199	0.1603	0.0253	0.1782	0.0181
8	0.1932	0.1702	0.1964	0.1138	0.1923	0.1219
9	0.1996	0.0309	0.2017	0.0093	0.1947	0.0125
10	0.2762	0.1495	0.2764	0.1339	0.2755	0.0720

[a] All values are given in electronvolts. The value of ΔG corresponds to the low-energy band.

TABLE 2: Solvent Relaxation Times in ps, τ_i, and Weights, x_i

solvent	τ_1	τ_2	x_1	x_2
ACN	0.19	0.50[a]	0.5	0.5
VaCN	0.19	4.7[b]	0.5	0.5
OcCN	0.19	6.4[b]	0.23	0.77

[a] Reference 11. [b] Reference 31.

difference in the free energies is equal to the band splitting). On the other hand, the charge transfer absorption band of the HMB/TCNE DAC is most probably due to a single transition.[6,52]

The results of the fit to the absorption spectra are depicted in Figure 2, and the corresponding parameters as well as the frequencies of the Franck−Condon active modes are listed in Table 1. Our data for HMB/TCNE are slightly different from those obtained in ref 6 because of a different handling of the intramolecular mode with frequency $\hbar\Omega_0 = 0.021$ eV, which is considered here to be classical.

The quality of the fit of eq 11 to the absorption spectra is excellent for all DACs. Moreover, a special investigation has shown the set of resulting parameters to be unique.

Simulation of the Charge Recombination Dynamics. All simulations were performed at room temperature, $T = 300$ K, and the relaxation time constants of all quantum vibrational modes with $n \neq 0$ were the same and equal to $\tau_v^{(n)} = 150$ fs. The dynamic parameters of the solvents are listed in Table 2. The single unknown parameter, V_{el}, has been determined for each complex from the fit to the CR dynamics in VaCN upon 530 nm excitation. An example of such a fit for IDU/TCNE in VaCN is illustrated in Figure 3. The most important parameters obtained in the simulations are listed in Table 3 together with the experimental data[17] for comparison. The nonexponentiality parameter s was calculated from the fit of the decay of the DAC excited-state population, $P(t)$, to the trial function

$$f(t) = \exp\{-(t/\tau)^s\} \tag{3.2}$$

For $s < 1$, this function is known as the stretch exponential function. It is widely used to describe systems exhibiting relaxation occurring on a large range of time scales.[53]

The effective CR time constant was determined with the equation

$$\tau_{\text{eff}} = \int_0^\infty P(t)\, \mathrm{d}t \tag{3.3}$$

TABLE 3: Electronic Coupling, V_{el} in eV, Excitation Wavelength, λ_e in nm, Nonexponentiality Factor, s, Effective CR Time Constants, τ_{eff} in ps, and Spectral Effect, ϕ[a]

DAC	solvent	λ_e	s^{exp}	s^{num}	$\tau_{\text{eff}}^{\text{exp}}$	$\tau_{\text{eff}}^{\text{num}}$	ϕ^{exp}	ϕ^{num}
IDU/TCNE	ACN	480	1.3	1.68	0.80	0.95	0	−0,25
$V_{\text{el}} = 0.091$		530		1.66		0.88		
		620		1.60		0.71		
	VaCN	480	1.57	1.47	2.45	2.63	−0.16	−0.44
		530	1.53	1.40	2.25	2.25		
		620	1.30	1.24	2.03	1.47		
	OcCN	480	1.46	1.99	5.52	5.27	−0.09	−0.25
		530	1.35	1.86	5.14	4.56		
		620	1.28	1.53	5.04	2.94		
PMB/TCNE	ACN	480	1.3	2.06	0.55	0.74	0	−0.23
$V_{\text{el}} = 0.113$		530		2.00		0.69		
		620		1.89		0.57		
	VaCN	480	1.35	1.57	1.95	2.25	0	−0.42
		530		1.47		1.94		
		620		1.31		1.30		
	OcCN	480	1.25	2.26	3.8	5.04	0	−0.40
		530		2.12		4.43		
		620		1.76		3.04		
HMB/TCNE	ACN	480	1.3	2.46	0.45	0.54	0	−0.15
$V_{\text{el}} = 0.143$		530		2.40		0.52		
		620		2.17		0.46		
	VaCN	480	1.31	1.59	1.35	1.55	0.081	−0.33
		530	1.26	1.50	1.39	1.39		
		620	1.14	1.37	1.46	1.04		
	OcCN	480	1.17	2.41	2.62	4.05	0	−0.32
		530		2.25		3.68		
		620		1.85		2.74		

[a] The superscripts exp and num refer to experimental[17] and theoretical results, respectively.

The spectral effect is defined here as

$$\phi = \frac{\tau_{\text{eff}}^{620} - \tau_{\text{eff}}^{480}}{\tau_{\text{eff}}^{480}} \tag{3.4}$$

where the superscript indicates the excitation wavelength in nanometers.

Electronic Coupling. The electronic couplings associated with all DACs are rather close to each other (see Table 3). This result is natural considering the similarity of the three complexes and the fact that the intensities of their charge transfer absorption bands are nearly equal. It should be noted that other estimates of this quantity have been reported in refs 6 and 54 and are rather close to that obtained here.

Naturally, the large value of the electronic coupling $V_{el} = 0.143$ eV for HMB/TCNE raises a question about the applicability of the nonadiabatic model used in this paper. The formal applicability condition for the stochastic approach is $V_{el} < k_B T$.[44] However, one should keep in view that within the multi-sink model (eqs 2.4 and 2.5) this large value of V_{el} is not actually concentrated at a single intersection point but rather "spread" over a large number of term intersections, where these couplings are effectively suppressed by the Franck−Condon factors F_n (eq 2.8). To illustrate the importance of these factors in ultrafast charge recombination, we have pictured in Figure 4 the values of F_n and the probabilities of nonthermal electronic transition through the corresponding sinks, Y_n, for the HMB/TCNE complex. The figure shows all probabilities, Y_n, to be less than 0.025. Such small values of Y_n provide evidence that the transitions proceed in the nonadiabatic regime. Notice, for larger values of the electronic coupling, when the solvent-controlled regime is reached, the magnitudes of Y_n should, at least, be larger by a factor of 10.[13]

Analysis of the data presented in Figure 4 shows that about half of all electronic transitions proceed through the sinks with

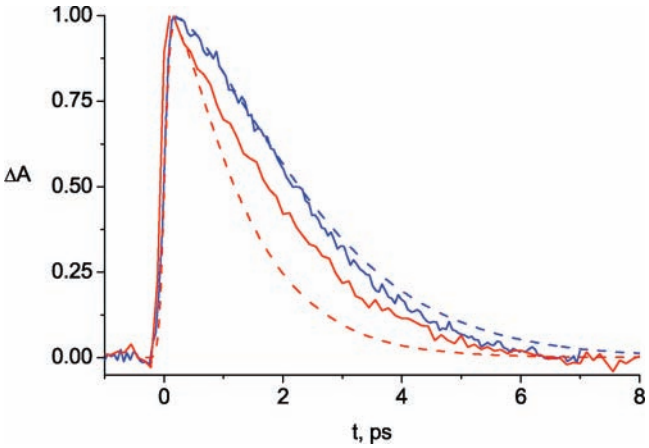

Figure 3. CR dynamics of the IDU/TCNE DAC in VaCN. Experimental data (solid lines) and simulation results (dashed lines). The color of the line indicates excitation wavelength (red, 620 nm; blue, 480 nm).

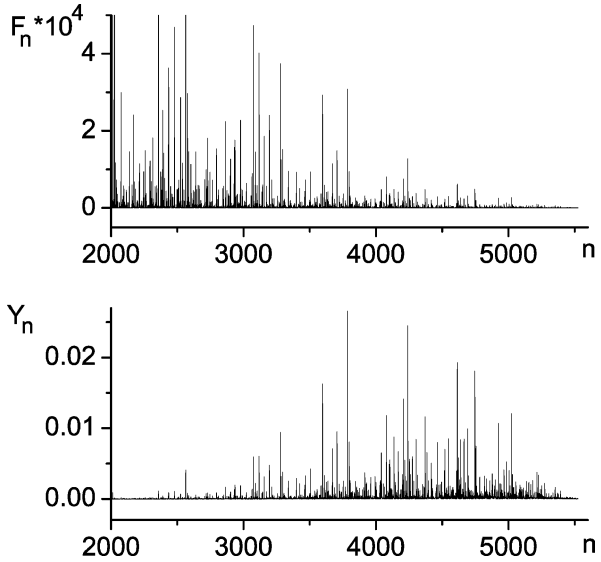

Figure 4. Franck−Condon factors, F_n, and quantum yields, Y_n, as a function of the crossing point number. The results are obtained from simulations of the CR dynamics for HMB/TCNE in VaCN solution after excitation at 620 nm.

F_n smaller than 10^{-4}, which are located rather far from the most effective sinks. The maximal values of the hot transitions probability are achieved at the sinks with $F_n \simeq 10^{-4}$. Upon further motion, the wave packet passes through more effective sinks with smaller n and considerably larger magnitudes of F_n. However, the occupation of the corresponding sublevels goes down due to the depopulation of the excited state. The transitions are practically terminated when the wave packet reaches the sinks with $n \approx 2300$ and $F_n = 5 \times 10^{-4}$. As a consequence, the wave packet never reaches the bottom of the excited-state well which is located near the sink with $n = 2024$; that is, all transitions proceed in nonthermal regime. The effective electronic couplings for all sinks actually participating in the nonthermal transitions is $V_n < 0.0032$ eV, justifying the applicability of the model used. For the IDU/TCNE and PMB/TCNE complexes, the maximum values of V_n are even smaller.

The above results pronouncedly provide evidence for the crucial role of the reorganization of the intramolecular high-frequency vibrational modes in ultrafast CR of excited DACs. This is conditioned by a large number of active intracomplex vibrational modes that result in a huge number of weak sinks on the excited-state free energy surface. Despite the sinks weakness, the total transition probability approaches unity because of their vast number. Simulations have shown that about 3000 vibrational sublevels of the ground state are populated.

Nonexponentiality Parameter. The theory considered in this paper predicts this parameter to be $s > 1$ in full accord with the experimental data. Various simulated trends of the nonexponentiality factor behavior are in good qualitative agreement with the experimental observations. For example, theory predicts an increase of the nonexponentiality factor with the decrease of the excitation wavelength, as found experimentally. However, the values of the nonexponentiality parameter obtained from the theoretical simulation are considerably larger than those found in the experiments. The theoretical values in ACN and OcCN are overestimated by a factor 1.2−2. A satisfactory quantitative agreement between theoretical and experimental data is only found in VaCN.

Solvent Effect. A good correlation between experimental and calculated results is obtained with IDU/TCNE in all solvents. With PMB/TCNE and HMB/TCNE on the other hand, the model describes correctly the variation of the effective time constant in ACN and VaCN but overestimates it noticeably in OcCN.

In the simulations, the relative weights of the fast (inertial) and slow (diffusive) components in ACN and VaCN were set to $x_1 = x_2 = 0.5$. With such parameters, the CR time constant in OcCN is considerably underestimated. After having changed these parameters to $x_1 = 0.23$ and $x_2 = 0.77$, the solvent effect observed experimentally with the CR of IDU/TCNE upon 530 nm excitation could be well reproduced by the simulations in all three solvents.

Table 3 shows that there is also a really good accordance with the experimental data for PMB/TCNE and HMB/TCNE in ACN and VaCN. However, the CR time constant in OcCN is overestimated by a factor of 1.2−1.4.

In this work, the energetic parameters of the electron-transfer obtained from the fit to the stationary charge-transfer absorption band in ACN are supposed to be the same in all three solvents. This assumption may be incorrect for OcCN, which is markedly less polar than ACN and VaCN. Because of this, the driving force for CR in OcCN is most probably substantially larger than in the other solvents, and thus, CR might be intrinsically slower. Therefore, this difference, which has not been taken into account in the model, may play an important role in the solvent effect and perhaps in the spectral effect as well.

Spectral Effect. Only the spectral effect measured with IDU/TCNE could be correctly reproduced by the theoretical simulations. However, ϕ is overestimated by a factor 2.75 in VaCN and by an even larger value in the other solvents. Obviously, the theory is not applicable for describing the spectral effect with PMB/TCNE and HMB/TCNE. It even predicts an incorrect sign of the spectral effect for HMB/TCNE. Despite this, the model reproduces correctly the increase of ϕ by going from IDU/TCNE to PMB/TCNE and to HMB/TCNE.

It is known that the charge transfer absorption of HMB/TCNE can be complicated by the presence of two transitions involving the degenerate HOMOs of HMB.[55] This HOMO degeneracy in free HMB is expected to be broken upon complexation with an acceptor. In this case, the HMB/TCNE charge-transfer spectrum should consist of two transitions with a small energy splitting. In the calculations, a value of 0.15 eV has been used for the energy splitting. We tried to reproduce the positive spectral effect measured with the HMB/TCNE complex by supposing that the charge-transfer band includes two transitions of different intensities and that these intensities are proportional to the square

of the electronic coupling of the corresponding transition. Although the quality of the fit to the absorption spectrum appeared to be good with various intensities of the transitions, the positive spectral effect could not be reproduced. Moreover, this two-band model led to much larger values of the electronic coupling, in contradiction with the experimental data which indicates that the electronic coupling for HMB/TCNE is close to that of IDU/TCNE and PMB/TCNE.

IV. Concluding Remarks

In this paper, we have attempted to reproduce the CR dynamics of excited DACs and the dependencies of the effective CR rate constant on both the solvent relaxation times and the excitation pulse carrier frequency within the framework of a nonadiabatic stochastic model. This model turned out to be globally satisfactory for the IDU/TCNE complex, although it noticeably overestimates the spectral effect. For the PMB/TCNE and HMB/TCNE complexes, the model has been able to predict the solvent effect correctly but has failed to reproduce the spectral effect. Even an incorrect sign of the spectral effect has been obtained for the HMB/TCNE DAC. This failure raises questions on the changes that have to be brought to the model to give a satisfactory prediction of the spectral effect in this case too. At first glance, the large value of electronic coupling $V_{el} = 0.143$ eV obtained for this complex indicates that the reaction proceeds in the strong electronic coupling regime; hence, the Frantsuzov−Tachiya model or its nonstationary generalizations could be more appropriate. However, there are two reasons why such models of the HMB/TCNE complex should be rejected. First, the effective electronic couplings are greatly reduced by the Franck−Condon factors for all controlling sinks so that the weak electronic coupling limit is realized. Second, the investigations of the strong electronic coupling model have shown that only negative spectral effects can be expected in this case.[16]

The failure of the theory to describe the spectral effect can be elucidated if one takes into account experimental investigations by Mataga and co-workers.[56,57] Their data suggest that the Franck−Condon state of the excited DAC is characterized by partial charge separation and evolves into a contact ion pair with full charge separation. This suggestion is also supported by the observation of an anomalous increases of charge-transfer oscillator strength with increasing the oxidation potential of the donor. This result is in contradiction with the predictions of the two-state model and was explained by the contribution from localized excited states.[58] In accord with this explanation, the Franck−Condon state has to be relatively weakly ionic and an increase of ionicity should be expected upon intracomplex relaxation. Significantly, smaller value of the electronic coupling between the emitting states relative to the absorbing states observed experimentally in HMB/TCNE complexes[55] reinforce this hypothesis. Furthermore, very recent femtosecond transient absorption measurements with a DAC composed of methylperylene and TCNE in polar solvents indeed reveal an early excited-state with an incomplete charge-transfer character.[59] So, a three-level scheme (the ground state, two excited states with partial and full charge separation) may thus be more realistic to describe CR. Naturally, whether the transformation of the Franck−Condon state into a contact ion pair can be described as a transition between two electronic states is questionable. However, an important consequence of this is that, contrary to a two-level model, a three-level model may exhibit a positive spectral effect in the Marcus inverted region, $-\Delta G_{CR} > E_r$,[60,61] as observed for the HMB/TCNE complex.

The investigation described in this paper has shown that the model considered provides a qualitatively correct description of all experimentally observed trends but that there is a considerable quantitative disagreement. This result is rather natural because of some crudenesses in the model. Indeed, the simplest model of molecular vibrations has been used, neglecting the difference of the vibrational frequencies in the ground and excited electronic states, the Dushinski effect, and the anharmonicity of the vibrations. Each of these features can considerably change the value of the Franck−Condon factor for transitions with the creation of many vibrational quanta.[62] Since such transitions play a crucial role in the CR, a model taking all of these effects into account can be expected to better reproduce the experimental data.

Acknowledgment. This work was supported by the Russian foundation for basic research (Grant 07-03-96600) and by the Swiss National Science Foundation (Grant 200020-115942).

References and Notes

(1) Asahi, T.; Mataga, N. *J. Phys. Chem.* **1989**, *93*, 6575.
(2) Asahi, T.; Mataga, N. *J. Phys. Chem.* **1991**, *95*, 1956.
(3) Segawa, H.; Takehara, C.; Honda, K.; Shimidzu, T.; Asahi, T.; Mataga, N. *J. Phys. Chem.* **1992**, *99*, 503.
(4) Benniston, C. A.; Harriman, A.; Philp, D.; Stoddart, J. F. *J. Am. Chem. Soc.* **1993**, *115*, 5298.
(5) Gould, I. R.; Noukakis, D.; Gomez-Jahn, L.; Goodman, J. L.; Farid, S. *J. Am. Chem. Soc.* **1993**, *115*, 4405.
(6) Wynne, K.; Galli, C.; Hochstrasser, R. M. *J. Chem. Phys.* **1994**, *100*, 4797.
(7) Wynne, K.; Reid, G. D.; Hochstrasser, R. M. *J. Chem. Phys.* **1996**, *105*, 2287.
(8) Hubig, S. M.; Bockman, T. M.; Kochi, J. K. *J. Am. Chem. Soc.* **1996**, *118*, 3842.
(9) Nicolet, O.; Vauthey, E. *J. Phys. Chem. A* **2002**, *106*, 5553.
(10) Tachiya, M.; Murata, S. *J. Am. Chem. Soc.* **1994**, *116*, 2434.
(11) Walker, G. C.; Akesson, E.; Johnson, A. E.; Levinger, N. E.; Barbara, P. F. *J. Phys. Chem.* **1992**, *96*, 3728.
(12) Bagchi, B.; Gayathri, N. *Adv. Chem. Phys.* **1999**, *107*, 1.
(13) Ivanov, A. I.; Potovoi, V. V. *Chem. Phys.* **1999**, *247*, 245.
(14) Ivanov, A. I.; Belikeev, F. N.; Fedunov, R. G.; Vauthey, E. *Chem. Phys. Lett.* **2003**, *372*, 73.
(15) Fedunov, R. G.; Feskov, S. V.; Ivanov, A. I.; Nicolet, O.; Pagès, S.; Vauthey, E. *J. Chem. Phys.* **2004**, *121*, 3643.
(16) Mikhailova, V. A.; Ivanov, A. I.; Vauthey, E. *J. Chem. Phys.* **2004**, *121*, 6463.
(17) Nicolet, O.; Banerji, N.; Pagès, S.; Vauthey, E. *J. Phys. Chem. A* **2005**, *109*, 8236.
(18) Frantsuzov, P. A.; Tachiya, M. *J. Chem. Phys.* **2000**, *112*, 4216.
(19) Feskov, S. V.; Ionkin, V. N.; Ivanov, A. I. *J. Phys. Chem. A* **2006**, *110*, 11919.
(20) Jortner, J.; Bixon, M. *J. Chem. Phys.* **1988**, *88*, 167.
(21) Barbara, P. F.; Walker, G. C.; Smith, T. P. *Science* **1992**, *256*, 975.
(22) Denny, R. A.; Bagchi, B.; Barbara, P. F. *J. Chem. Phys.* **2001**, *115*, 6058.
(23) Mikhailova, V. A.; Ivanov, A. I. *J. Phys. Chem. C* **2007**, *111*, 4445.
(24) Sumi, H.; Marcus, R. A. *J. Chem. Phys.* **1986**, *84*, 4272.
(25) Zusman, L. D. *Chem. Phys.* **1980**, *49*, 295.
(26) Burshtein, A. I.; Yakobson, B. I. *Chem. Phys.* **1980**, *49*, 385.
(27) Garg, S.; Smith, C. *J. Phys. Chem.* **1965**, *69*, 1294.
(28) Rosenthal, S. J.; Xie, X.; Du, M.; Fleming, G. R. *J. Chem. Phys.* **1991**, *95*, 4715.
(29) Maroncelli, M.; Kumar, V. P.; Papazyan, A. *J. Phys. Chem.* **1993**, *97*, 13.
(30) Jimenez, R.; Fleming, G. R.; Kumar, P. V.; Maroncelli, M. *Nature* **1994**, *369*, 471.
(31) Gumy, J. C.; Nicolet, O.; Vauthey, E. *J. Phys. Chem. A* **1999**, *103*, 10737.
(32) Bakhshiev, N. G. *Opt. Spectrosc. (USSR)* **1964**, *16*, 446.
(33) Hizhnyakov, V.; Tekhver, Yu, I. *Phys. Status Solidi* **1967**, *21*, 75.
(34) Mazurenko, Yu.-T.; Bakhshiev, N. G. *Opt. Spectrosc. (USSR)* **1970**, *28*, 490.
(35) Zusman, L. D.; Helman, A. B. *Opt. Spectrosc. (USSR)* **1982**, *53*, 248.
(36) Bagchi, B.; Oxtoby, D. W.; Fleming, G. R. *Chem. Phys.* **1984**, *86*, 25.
(37) Van der Zwan, G.; Hynes, J. T. *J. Phys. Chem.* **1985**, *89*, 4181.

(38) Loring, R. F.; Yan, Y. J.; Mukamel, S. *J. Chem. Phys.* **1987**, *87*, 5840.
(39) Najbar, J.; Dorfman, R. C.; Fayer, M. D. *J. Chem. Phys.* **1991**, *94*, 1081.
(40) Coalson, R. D.; Evans, D. G.; Nitzan, A. *J. Chem. Phys.* **1994**, *101*, 436.
(41) Cho, M.; Silbey, R. J. *J. Chem. Phys.* **1995**, *103*, 595.
(42) Domcke, W.; Stock, G. *Adv. Chem. Phys.* **1997**, *100*, 1.
(43) Jean, J. M. *J. Phys. Chem. A* **1998**, *102*, 7549.
(44) Barzykin, A. V.; Frantsuzov, P. A.; Seki, K.; Tachiya, M. *Adv. Chem. Phys.* **2002**, *123*, 511.
(45) Gladkikh, V.; Burshtein, A. I.; Feskov, S. V.; Ivanov, A. I.; Vauthey, E. *J. Chem. Phys.* **2005**, *123*, 244510.
(46) Gould, I. R.; Noukakis, D.; Gomez-Jahn, L.; Young, R. H.; Goodman, J. L.; Farid, S. *J. Am. Chem. Soc.* **1993**, *115*, 3830.
(47) Gould, I. R.; Noukakis, D.; Goodman, J. L.; Young, R. H.; Farid, S. *Chem. Phys.* **1993**, *176*, 439.
(48) Gomes, S.; Hagemann, H.; Yvon, K. *J. Alloys Compd.* **2002**, *346*, 206.
(49) Markel, F.; Ferris, N. S.; Gould, I. R.; Myers, A. B. *J. Am. Chem. Soc.* **1992**, *114*, 6208.
(50) Kulinowski, K.; Gould, I. R.; Myers, A. B. *J. Phys. Chem.* **1995**, *99*, 9017.
(51) Voigt, E. M *J. Am. Chem. Soc.* **1964**, *86*, 3611.
(52) Rossi, M.; Buser, U.; Haselbach, E. *Helv. Chim. Acta* **1976**, *59*, 1039.
(53) Edholm, O.; Blomberg, C. *Chem. Phys.* **1999**, *252*, 221.
(54) Jurgensen, C. W.; Peanasky, M. J.; Drickamer, H. G. *J. Chem. Phys.* **1985**, *83*, 6108.
(55) Myers, Kelly, A. *J. Phys. Chem. A* **1999**, *103*, 6891.
(56) Asahi, T.; Ohkohchi, M.; Mataga, N. *J. Phys. Chem.* **1993**, *97*, 13132.
(57) Mataga, N.; Miyasaka, H. *Adv. Chem. Phys.* **1999**, *107*, 431.
(58) Foster, R. *Organic Charge-Transfer Complexes*; Academic Press: New York, 1969.
(59) Mohammed, O. F.; Vauthey, E., manuscript in preparation.
(60) Fedunov, R. G.; Ivanov, A. I. *J. Chem. Phys.* **2005**, *122*, 064501.
(61) Khohlova, S. S.; Mikhailova, V. A.; Ivanov, A. I. *J. Chem. Phys.* **2006**, *124*, 114507.
(62) Ivanov, A. I.; Ponomarev, O. A. *Opt. Spectrosc. (USSR)* **1976**, *41*, 744.